Korean J. Chem. Eng., 32(7), 1422-1426 (2015)
DOI: 10.1007/s11814-014-0344-4

pISSN: 0256-1115
eISSN: 1975-7220

Formation of compositional gradient profiles by using shear-induced polymer migration phenomenon under Couette flow field

Sang Hyuk Im*, Su Jin Lee*, Duck Jong Suh, O Ok Park**,†, and Moo Hyun Kwon*****

*Functional Crystallization Center, Department of Chemical Engineering, Kyung Hee University, 1732, Deogyeong-daero, Giheung-gu, Yongin-si, Gyeonggi 446-701, Korea
**Department of Chemical and Biomolecular Engineering (BK21+ Graduate Program), Korea Advanced Institute of Science and Technology (KAIST), 291, Daehak-ro, Yuseong-gu, Daejeon 305-701, Korea
***Department of Applied Chemistry, Woosuk University, 443, Samrae-ro, Sangrae-eup, Wanju-gun, Jeonbuk 565-701, Korea
(*Received 10 June 2014 • accepted 23 November 2014*)

Abstract−We investigated whether a graded-index profile, specified by the polymer compositional gradient, could be formed using shear-induced polymer migration phenomenon in a polymer solution. For the presented model system, we generated a shear flow by rotating a glass rod at the center of a polystyrene/methylmethacrylate (PS/MMA) solution and measured the degree of polymer migration by the shear flow field by examining the concentration of polymer solution along the radial direction from the rotating axis to the periphery. Through model experiments, we formed a compositional gradient and controlled its profile in the solution by varying the concentration of polymer solution, molecular weight of polymer, and shear rate. Finally, we solidfied the gradient profiles by the polymerization of the PS/MMA solution and confirmed that the gradient profiles were maintained with a compositional gradient twice larger than the mother PS/MMA solution.

Keywords: Graded Index, Compositional Gradient, Polymer Migration, Polymer Optical Fiber

INTRODUCTION

Techniques for forming a graded-index refractive-index (GI) profile, as indicated by chemical compositional gradient, have been intensively studied [1-4], because a GI profile is essential in the fabrication of polymeric lenses, image guides, and optical fibers to obtain clear images or information without distortion.

In particular, optical fibers have begun to be greatly noticed with rapidly increasing demands in the communication industry. Single-mode, step-index glass optical fibers (SMSI-GOFs) have been commercialized for high-speed communication. Optical fibers can efficiently guide and utilize a light source; however, the inherent brittleness of glass materials limits their application in uses requiring flexibility and frequent connection in buildings. Therefore, multimode, graded-index polymer optical fibers (MMGI-POFs) are better candidates to exploit solar energy because they can guide more light, owing to larger diameters. Such fibers can also be woven into solar fabrics, such as organic solar cells [5-7] or sensitized solar cells [8], due to their good flexibility.

To date, GI profiles have been constructed via interfacial gel polymerization [2-4], co-extrusion [9], polymerization under ultra-centrifugal force [10-12], and laminar shear mixing [13]. Interfacial gel polymerization utilizes the bulky dopants with higher refractive index than the polymerizing materials. The polymerization occurs in a polymeric tube, which makes a gel-like monomer-polymer interface so that the unreactive bulky dopants are gradually concentrated to the center axis during the polymerization. However, the long-term stability of the GI profile has some problem by the migration of bulky dopants. The co-extrusion method continuously co-extrudes the core and the shell polymeric material with high and low refractive index, respectively. It can continuously make fiber type a product with GI profile, but the profile is not reliably formed due to the difficulty of interdiffusion of polymer melts. The polymerization under ultra-centrifugal force uses two monomers with different density and refractive index so that the concentration profile is formed by the density profile under centrifugal force field. It can make a reliable GI profile and has long-term stability because it does not require dopants. However, a cavity along the rotating axis is inevitably formed so that an additional feeding process or special reactor design is needed to compensate the cavity during the polymerization. The laminar shear mixing method is to form the concentration profile by rotating polymeric rod with higher refractive index in a reactive monomer solution with lower refractive index. By the rotating process, the monomer is diffused in the polymeric rod, and consequently makes monomer swollen polymeric rod. The concentration profile is then fixed by the polymerization. However, it is difficult to control the GI profile shape and the profile can be disturbed by the dissolved polymer in the monomer. In the present work, we added an additional method to form the GI profiles by using shear-induced polymer migration phenomena.

Shear-flow-induced polymer migration phenomena involving rigid rods or particles in a polymer solution have been reported [14-17],

†To whom correspondence should be addressed.
E-mail: ookpark@kaist.ac.kr
‡This article is dedicated to Prof. Hwayong Kim on the occasion of his retirement from Seoul National Univerisity.

and the existence of such migration has been verified. MacDonald et al. reported on shear-induced polymer migration phenomena involving a dilute solution with a rotating cone-and-plate configuration [18,19]. Criado-Sancho et al. provided theoretical models to explain the shear-induced polymer migration phenomenon [20,21].

To form GI profiles applicable to the fabrication of polymeric lenses or optical fibers, in the present work, we adopted a cylindrical configuration and polymerized highly concentrated polystyrene/methylmethacrylate (PS/MMA) solution for a model system. We systematically examined the variation of compositional profiles according to the concentration of the polymer solution, the molecular weight of the polymer, the shear rate, and the polymerization.

EXPERIMENTAL PROCEDURE

1. Materials

A low-molecular weight (LMW) PS (Aldrich, Mw=45,000), a high-molecular weight (HMW) PS (Aldrich, Mw=350,000), and an MMA (Aldrich) were used as received.

2. Procedure

A 5 wt% LMW-PS/MMA solution was charged in a glass tube (inner diameter=42 mm), and a glass rod (diameter=5 mm) was rotated at 60 rpm in the polymer solution. After 5 hr, samples from varying radial distance were chosen for H^1-NMR analysis to analyze the concentration profiles [11,12]. Similarly, samples were chosen from 10 wt%, 20 wt%, and 30 wt% LMW-PS/MMA solutions and from 10 wt%, 20 wt%, and 26 wt% HMW-PS/MMA solutions. To examine the variations of the concentration profiles with repect to shear rate, samples were chosen by four points along with radial direction in 30, 60, 120 rpm sample, respectively, in a 20 wt% HMW-PS/MMA solution. Finally, the 20 wt% HMW-PS/MMA solution was polymerized at 65 °C for 24 h via two different methods: (1) a sequential method, whereby before polymerization the compositional gradient was formed by rotating the glass rod for 5 h; (2) a simultaneous method, which omitted the forming process of the compositional gradient.

RESULTS AND DISCUSSION

Fig. 1 shows photographs of the presented model system configuration, in which a glass rod (d=5 mm) was rotated at 60 rpm in a cylindrical glass vessel (inner diameter=42 mm) containing a polymer solution. The rotating rod generated shear flow similar to a Couette flow with a configuration of wide separation gap. The apparent flow velocity near the vicinity of the rod was the same as the rotating speed of the glass rod and sharply decreased with radial direction.

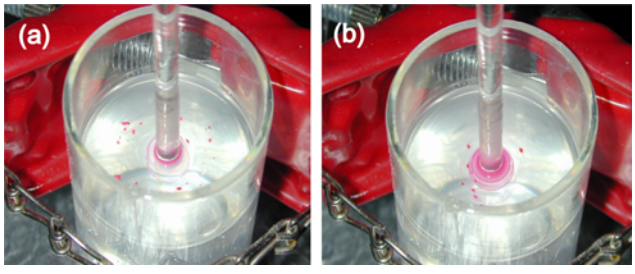

Fig. 1. Photographs of the model experiment for shear-induced polymer migration in a 26 wt% of HMW-PS/MMA solution: (a) upon adding a red dye powder to the solution and (b) after 5 min. Conditions were as follows: rotating glass rod speed=60 rpm, diameter of rod=5 mm, and inner diameter of cylindrical vessel=42 mm.

To observe the flow direction in the model system, we added a red dye powder, as shown in Fig. 1(a). As expected, the red dye migrated in an inward direction and gathered around the rotating rod, as shown in Fig. 1(b). This implies that polymers migrate via a shear-induced flow and that the direction of the migration is inward. The overall flux of a polymer chain in a polymer solution can be expressed as [18]:

$$\text{Flux of polymer} = -\mathbf{D}_{tr}\nabla\mathbf{n} - (\mathbf{D}_{tr}/\mathbf{kT})\nabla \bullet \tau_p \quad (1)$$

where τ_p is the symmetric second-order tensor, representing the polymeric contribution to the stress, k is Boltzmann's constant, T is temperature, D_{tr} is the translational diffusivity, and n is the polymer concentration. The first term represents Fickian diffusion due to concentration gradients, and the second term represents a migration caused by the elastic contribution to the stress tensor. Therefore, the concentration profile will be mainly affected by the second term ($\nabla \bullet \tau_p$). The value of $\nabla \bullet \tau_p$ is expressed as follows [18]:

$$\nabla \bullet \tau_p = \lambda \tau_p : \nabla\nabla\mathbf{v} \quad (2)$$

where $\lambda = 6[\eta]M\eta_s/\pi^2 N_A kT$ is the longest relaxation time. Accordingly, N_A is Avogadro's number, $[\eta]$ is the intrinsic viscosity of the polymer in a solvent, M is molecular weight, η_s is the viscosity of a solvent, and $\tau_p = \eta\gamma^*$ (in Newtonian fluid; η=the viscosity of a solution and γ^*=shear rate) is a stress. Hence, λ is a function of molecular weight, and τ_p is a function of the viscosity of the polymer solution and shear rate. From Eq. (2), it is expected that the concentration profile depends on the concentration of the polymer solution, the molecular weight of polymer, and the shear rate.

The concentration difference (ΔC=wt fraction of PS in the solution at the sampling point - wt fraction of PS in the solution at the vicinity of inner cylindrical vessel) profiles of the PS concentration in an LMW-PS/MMA and an HMW-PS/MMA solution are plotted in Fig. 2 because the refractive index has a linear relationship to the wt fraction of PS in the PS/MMA solution [11]. The representative H^1-NMR spectrum of PS/MMA solution is shown in Fig. 2(a). The composition was calculated by comparing the integrated value of phenyl group in PS and hydrogen in MMA. In a LMW-PS/MMA solution, as shown in Fig. 2(b), the graded concentration profile did not appear in the relatively lower PS concentration solutions (5 wt% and 10 wt% LMW-PS/MMA solutions) because the elastic contribution to the stress tensor will be weak due to relatively lower solution viscosity (~3 mP·s and ~45 mP·s viscosity in 5 wt% and 10 wt% LMW-PS/MMA solution, respectively) and smaller PS chain length. However, graded concentration profiles appeared with solutions having over 20 wt% LMW-PS/MMA, owing to the strengthened elastic contribution to the stress tensor (~2,000 mP·s and ~11,000 mP·s viscosity in 20 wt% and 30 wt% LMW-PS/MMA solution, respectively). The ΔC value at the vicinity of the rotating rod increased with increased values of

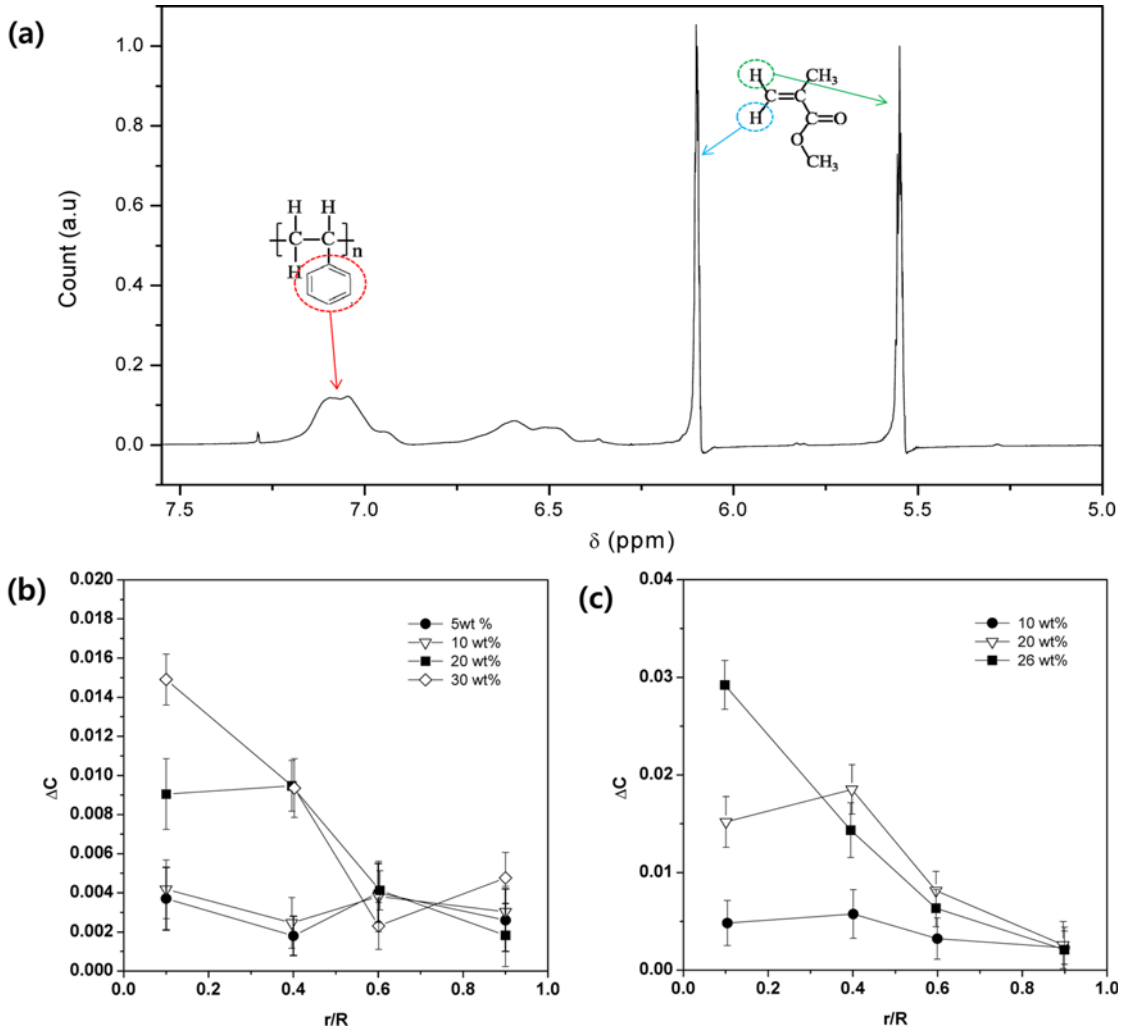

Fig. 2. (a) Representative H^1-NMR spectrum of PS/MMA solution; and The DC profiles using (b) an LMW-PS/MMA solution and (c) an HMW-PS/MMA solution with respective radial distances.

LMW-PS/MMA solution, and the ΔC profile shape was also controllable by simply adjusting the concentration of the polymer solution.

The ΔC profiles attained using the HMW-PS/MMA solution are shown in Fig. 2(c). A graded concentration profile was observed with the 10 wt% PS/MMA solution, while it was not observed using the 10 wt% LMW-PS/MMA solution. The ΔC between the rotating center and the periphery in the 26 wt% HMW-PS/MMA solution increased to almost twice that of the 20 wt% solution. The larger ΔC attained by using a HMW-PS/MMA solution compared to using an LMW-PS/MMA solution might be attributed to the increased intrinsic viscosity, which elongates the longest relaxation time and, consequently, increases the migration term.

To examine the ΔC with shear rate (rotating speed), we conducted experiments with a 20 wt% HMW-PS/MMA solution. Fig. 3 shows that the ΔC is higher as the shear rate is increased because the stress term has a linear correlation with the shear rate. As a result, the migration term is strengthened, leading to a larger ΔC difference with repect to the shear rate. Thus, we can conclude that the ΔC value and its profile can be controlled by manipulating the polymer molecular weight and the shear rate.

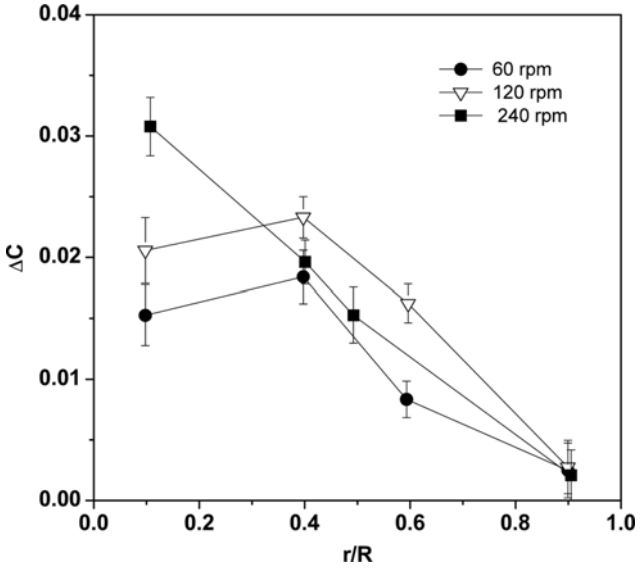

Fig. 3. The DC profiles with varying rotating speeds in a 20 wt% HMW-PS/MMA solution.

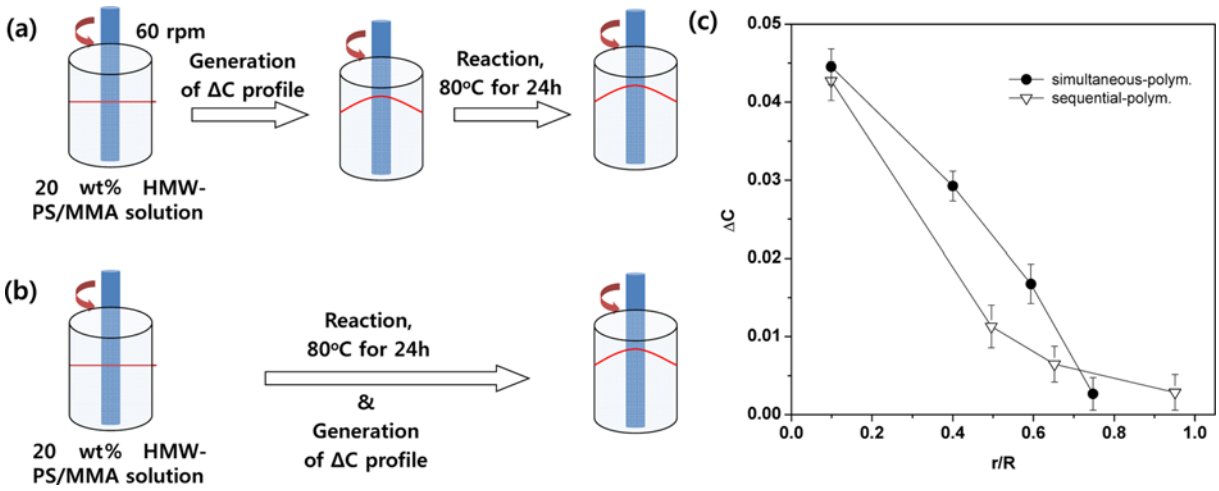

Fig. 4. Schematic illustration of (a) sequential polymerization, (b) simultaneous polymerization, and (c) the DC profiles with polymerization methods. Solutions of 20 wt% HMW-PS/MMA were used in both cases. In Fig. 4(c), the inverse triangles represent sequential polymerization, while the circles represent simultaneous polymerization.

To fabricate polymeric lenses or optical fiber preforms with graded refractive indices, the polymer solutions used should be changed to solid form. Therefore, we polymerized solutions with 0.4 wt% benzoyl peroxide (BPO) as an initiator at 80 °C for 24 h. If the polymer (in the present work, the polymethylmethacrylate (PMMA)) produced by the polymerization of the mother solution has a higher molecular weight than the pre-existent polymer (in the present work, the PS) in the mother solution, the concentration profile could be disturbed by the produced polymer because a polymer with a higher molecular weight migrates more strongly than a polymer with a lower molecular weight. To avoid this undesirable disturbance of the concentration profile, in the present study, we used 0.4 wt% BPO as an initiator because it produced a lower molecular weight of PMMA (125000) than the HMW-PS (350000) in the mother solution.

Finally, we examined whether the preferentially generated graded concentration profile in a solution state affects the formed concentration profile through the polymerization, as illustrated in Fig. 4(a) and (b). Hence, we performed two different experiments with a 20 wt% HMW-PS/MMA solution. First, we sequentially polymerized the mother solution, as follows: (1) formation of the graded concentration profile in a solution state, and (2) fixation of the graded concentration profile by polymerization. Second, we simultaneously polymerized the polymeric solution without forming a graded concentration profile in the solution state. Fig. 4(c) shows that the ΔC between the rotating center and the periphery was almost the same (0.04), and the ΔC values increased twice that of the solution state because the viscosity of the polymer solutions was increased. Consequently, the migration term was strenghthened.

Generally, the compositional graded profile can be expressed by Eq. (3) [11,12].

$$C(r/R)/C(r=0)=(1-2\Delta(r/R)^{\alpha})^{0.5} \quad (3)$$

where r is radial distance from the rotating axis, R is radius of the cylindrical vessel, Δ is (ΔC(r/R)/C(r=0), and the dimensionless parameter α is the shape of the compositional graded profile. When α is close to 2, the transmission rate of light is maximized. The Δ and α can be calculated from the interpolated value and slope of $\log\{1-(C(r/R)/C(r=0))^2\}$ vs log(r/R) graph. Roughly, the α value of the ΔC profile in sequential and simultaneous polymerization was ~2 and ~1.1, because the ΔC profile of the simultaneous polymerization is more stiffly decreased than that of sequential polymerization. The smoother ΔC profile of sequential polymerization might be attributed to the fact that the rate of polymerization around the center region of the solution is higher than that around the outer region of the solution, because polymerization in gel phase (polymer concentrated region around the rotating axis) proceeds faster than that in dilute phase (around the periphery). Accordingly, a preferentially formed ΔC profile (see Fig. 2(b)) in a solution state is maintained. The magnitude of the ΔC is only increased by the ΔC profile obtained in a 26 wt% HMW-PS/MMA solution (see Fig. 3) because of the similar resultant increase of a polymer's concentration. This implies that the compositional gradient profiles can be controlled via specific polymerization methods.

CONCLUSIONS

We have formed compositional gradient profiles by utilizing shear-induced polymer migration, and controlled their profile shapes by controlling the concentration of polymer solution, the polymer molecular weight, the shear rate, and the polymerization methods. Shear-induced polymer migration phenomena were observed in a PS/MMA solution with a cylindrical geometry. With the exception of 5 and 10 wt% in an LMW-PS/MMA solution, graded concentration profiles were observed in both LMW and HMW-PS/MMA solutions. The ΔC profiles of polymeric solutions were found to be controllable with the concentration of polymer solution and shear rate, because the stress imposed on the polymer chains causes the polymer chains in the solution to migrate toward the rotating axis Finally, we solidified polymer solutions using two different polymerization methods (simultaneous and sequential). We found that the ΔC profiles could be controllable by specific polymerization

methods.

ACKNOWLEDGEMENTS

This work was supported by the Basic Science Research Program (No.: NRF-2014R1A5A1009799) through the National Research Foundation of Korea (NRF) funded by the Ministry of Science, ICT & Future Planning.

REFERENCES

1. C. Emslie, *J. Mater. Sci.*, **23**, 2281 (1988).
2. Y. Koike, A. Kanemitsh, E. Nihei and Y. Ohtsuka, *Appl. Opt.*, **33**, 3394 (1994).
3. M. Sato, T. Ishigure and Y. Koike, *J. Lightwave Technol.*, **18**, 952 (2000).
4. T. Ishigure, E. Nihei and Y. Koike, *Appl. Opt.*, **35**, 2048 (1996).
5. D. Liu, M. Zhao, Y. Li, Z. Bian, L. Zhang, Y. Shang, X. Xia, S. Zhang, D. Yun, Z. Liu, A. Cao and C. Huang, *ACS Nano*, **6**, 11027 (2012).
6. J. Lee, A. Kim, S. M. Cho and H. Chae, *Korean J. Chem. Eng.*, **29**, 337 (2012).
7. N. T. N. Truong, M. L. Monroe, U. Farva, T. J. Anderson and C. Park, *Korean J. Chem. Eng.*, **28**, 1625 (2011).
8. S. Pan, Z. Yang, P. Chen, J. Deng, H. Li and H. Peng, *Angew. Chem. Int. Ed.* (2014), DOI:10.1002/anie.201402561.
9. C. W. Park, B. C. Lee, S. K. Wallker and W. Y. Choi, *Ind. Eng. Chem. Res.*, **39**, 79 (2000).
10. F. G. H. van Duijnhoven and C. W. M. Bastiaansen, *Appl. Opt.*, **38**, 1008 (1999).
11. S. H. Im, D. J. Suh, O. O. Park, H. Cho, J. S. Choi, J. K. Park and J. T. Hwang, *Appl. Opt.*, **41**, 1858 (2002).
12. S. H. Im, D. J. Suh, O. O. Park, H. Cho, J. S. Choi. J. K. Park and J. T. Hwang, *Korean J. Chem. Eng.*, **19**, 505 (2002).
13. J. S. Choi, S. H. Im, M. Y. Song, O. O. Park, H. Cho and J. T. Hwang, *J. Appl. Polym. Sci.*, **95**, 1100 (2005).
14. V. G. Mavrantzas and A. N. Beris, *Phys. Rev. Lett.*, **69**, 273 (1992).
15. A. N. Beris and V. G. Mavrantzas, *J. Rheol.*, **38**, 1235 (1994).
16. M. V. Apostolakis, V. G. Mavrantzas and A. N. Beris, *J. Non-Newtonian Fluid Mech.*, **102**, 409 (2002).
17. S. Tsouka, Y. Dimakopoulos, V. Mavrantzas and J. Tsamopoulos, *J. Rheol.*, **58**, 911 (2014).
18. M. J. MacDonald and S. J. Muller, *J. Rheol.*, **40**, 259 (1996).
19. M. J. MacDonald and S. J. Muller, *Rheol. Acta*, **36**, 97 (1997).
20. M. C. Sancho, D. Jou, L. F. del Castillo and J. C. Va'zquez, *Polymer*, **41**, 8425 (2000).
21. L. F. del Castillo, M. C. Sancho and D. Jou, *Polymer*, **41**, 2633 (2000).